

**THE SWEDISH RESEARCH COUNCILS' LABORATORY**

**Studsvik, Fack  
S-611 01 Nyköping 1  
Sweden**

**Research report  
LF-76  
1977**

---

**TOTAL  $\beta$ -DECAY ENERGIES AND MASSES OF STRONGLY NEUTRON-RICH  
INDIUM ISOTOPES RANGING FROM  $A = 120$  TO  $129$**

**K Aleklett<sup>\*</sup>, E Lund, and G Rudstam  
The Swedish Research Councils' Laboratory,  
Studsvik, Fack, S-611 01 Nyköping, Sweden**

**\* ) and Chalmers University of Technology, Göteborg, Sweden**

TOTAL  $\beta$ -DECAY ENERGIES AND MASSES OF STRONGLY NEUTRON-RICH INDIUM  
ISOTOPES RANGING FROM  $A = 120$  TO  $129$

K Aleklett\*, E Lund, and G Rudstam  
The Swedish Research Councils' Laboratory,  
Studsvik, Fack, S-611 01 Nyköping, Sweden

Abstract

Beta spectra have been measured and total  $\beta$ -decay energies have been deduced for strongly neutron-rich indium isotopes. Mass separated sources were produced at the OSIRIS on-line separator at Studsvik. By applying  $\beta$ - $\gamma$  coincidence methods,  $Q_{\beta}$ -values were determined for isomers of  $^{120-129}\text{In}$ . For these nuclei, the atomic mass excess could be derived, allowing the comparison of masses of neutron-rich unstable nuclei with predictions from mass formulae. The mean uncertainty of the experimental mass excesses is 0.12 MeV. The precision of the mass formulae chosen for the comparison varies widely with the mean deviation ranging from 0.12 to 1.39 MeV.

---

Key words: RADIOACTIVITY  $^{120-129}\text{In}$ ; Measured  $\beta$ -spectra for isomers, deduced total  $\beta$ -decay energies and atomic mass excesses, comparison with mass formulae. Mass-separated fission products.

---

\* ) and Chalmers University of Technology, Gothenburg, Sweden

## 1. INTRODUCTION

A fundamental property of the atomic nucleus is its mass. The ISOL-technique<sup>1)</sup> has made an increasing number of nuclides far from the region of  $\beta$ -stability available for mass determinations. The most accurate measurements of stable nuclides have been performed with mass-spectrometers, and recently such determinations of neutron-deficient rubidium isotopes were reported<sup>2)</sup> with the spectrometer connected to ISOLDE at CERN. The uncertainties of the latter measurements are reported to be 25 - 80 keV. So far, direct mass determinations are limited to a few elements with restrictions that no other isobars or isomers are allowed to be present in the samples. This means that accurate direct mass-determinations will be extremely difficult to perform for the neutron rich indium isotopes of interest in this work because of the presence of isomerism. The indirect method of determining the mass differences from nuclear decay energies ( $Q_{\beta}$ -values) has been adopted in the present study.

Beside the general importance of masses and  $Q_{\beta}$ -values, mass data of neutron-rich nuclides are of special interest as these data are essential for the construction of mass formulae used in the theories of nucleosynthesis<sup>3)</sup> and for predictions about superheavy elements.

The isotope-separator facility OSIRIS<sup>4)</sup> connected to the R2-0 reactor at Studsvik is an excellent tool for producing neutron-rich fission products. With this equipment it has been possible to study indium isotopes ranging from  $^{117}\text{In}$  to  $^{132}\text{In}$ <sup>5-11)</sup>. In this article  $Q_{\beta}$ -values and mass excesses covering the mass range 120 - 129 are presented. The technique used in these experiments is described in Section 2, and in Section 3 the results of the  $Q_{\beta}$ -measurements are reported. Finally, the experimental  $Q_{\beta}$ -values and corresponding mass excesses are compared with predictions from different mass formulae in Section 4.

## 2. EXPERIMENTAL TECHNIQUES

### 2.1 On-line mass separation and sample production

At the OSIRIS facility,<sup>4)</sup> indium isotopes are produced by thermal-neutron induced fission of  $^{235}\text{U}$ . A cylinder consisting of several layers of graphite cloth is impregnated with about 3 g of the

target material and enclosed in the ion source of the isotope separator<sup>12</sup>). The recoiling fission fragments are caught in the graphite, diffuse to the surface, evaporate and, finally, get ionized and separated in a 55° fringing-field type of magnet<sup>13</sup>). There is very slight element selection in the system, and the samples contain generally two or more isobars which have to be separated by a proper timing of the experiment and also by carefully choosing the coincidence conditions.

The activities were collected on tape, either in the collector chamber of the separator or at an external tape position at the end of a beam-line. The collector chamber tape system needed a transportation time of 3 s<sup>14</sup>), while the external tape system transports the sample to the detector system within 0.3 s.

In the present work the uranium target was irradiated in a neutron flux of about  $10^{10} n_{th} cm^{-2} sec^{-1}$  (the available neutron flux is  $4 \times 10^{11} n_{th} cm^{-2} sec^{-1}$ ).

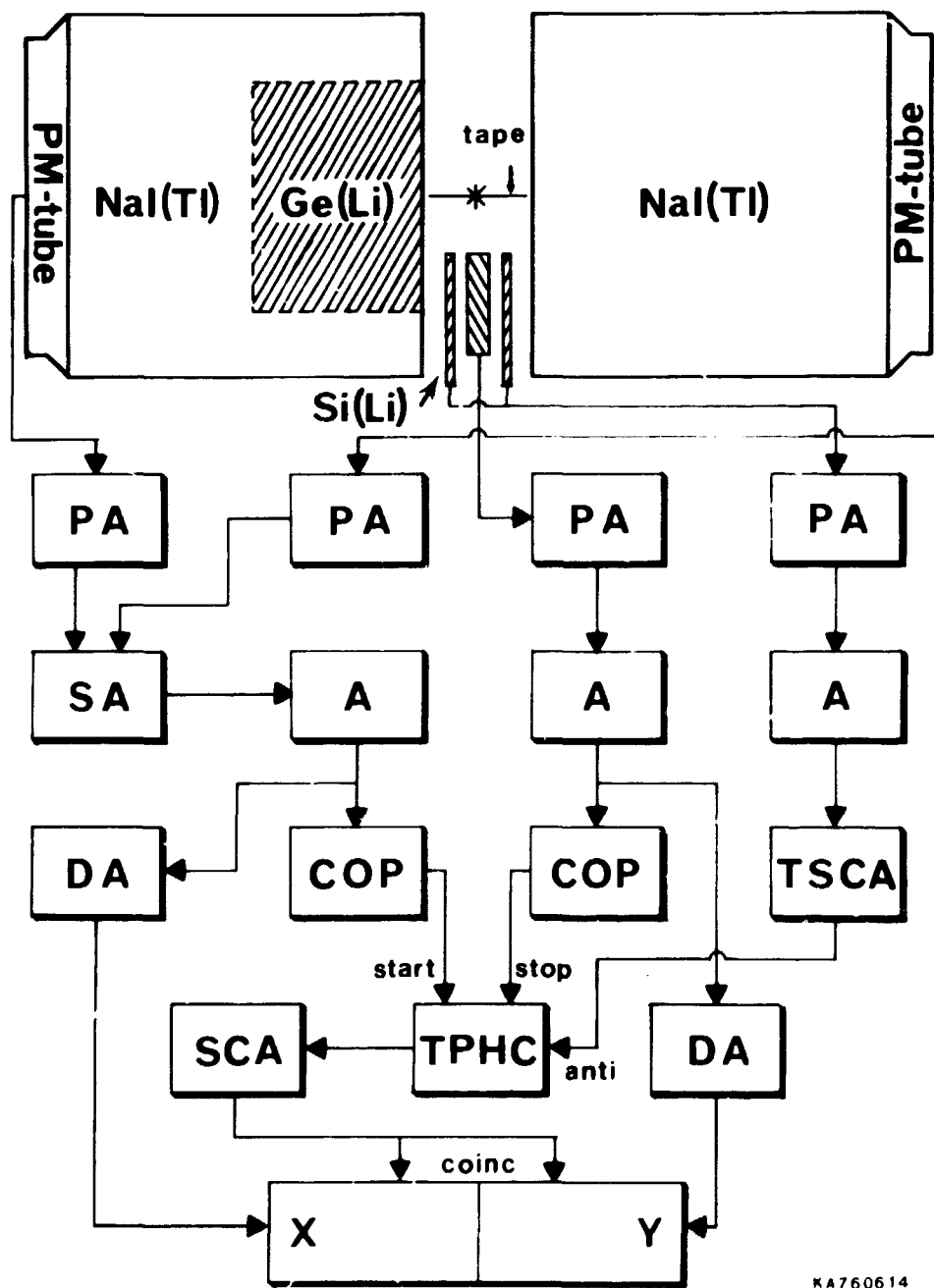
## 2.2 Detector arrangements

The basic principle for the determination of total  $\beta$ -decay energies is to measure  $\beta$ -branches to known excited states of the daughter nucleus. For this purpose a  $\beta$ - $\gamma$  coincidence spectrometer ( $Q_{\beta}$ -spectrometer) has been constructed. It consists of a system of Si(Li)-detectors for  $\beta$ -detection and two NaI(Tl)-detectors, or a Ge(Li)-detector, for  $\gamma$ -detection.

The  $Q_{\beta}$ -values reported in the present work are determined with the following detector configurations

Method I: <sup>120,121,124</sup>In; a main Si(Li)-detector surrounded by three anti-coincidence Si(Li)-detectors for  $\beta$ -detection and two NaI(Tl)-detectors for  $\gamma$ -detection; transport time 3 s.

Method II: <sup>126,127,128,129</sup>In; a main Si(Li)-detector surrounded by two anti-coincidence Si(Li)-detectors for  $\beta$ -detection and two NaI(Tl)-detectors for  $\gamma$ -detection; transport time 0.3 s.



KA760614

Fig 1. Block diagram of the electronics used for counting  $\beta$ - $\gamma$  coincidences with Method II. The Ge(Li)-detector used in Method III is also indicated. (PA = preamplifier; SA = sum amplifier; A = amplifier; DA = delay amplifier; COP = cross-over pickoff; TSCA = timing single channel analyzer; SCA = single channel analyzer; TPHC = time-to-pulse-height converter; X and Y = analog-to-digital converters)

Method III:  $^{122,123,124,125}\text{In}$ ; a main Si(Li)-detector surrounded by two anti-coincidence Si(Li)-detectors for  $\beta$ -detection and a Ge(Li)-detector for  $\gamma$ -detection; transport time 0.3 s.

In all experiments the same main Si(Li)-detector was used: a 25 mm dia x 5 mm thick transmission detector from which a segment has been cut in such a way that the  $\beta$ -particles from a sample will see a sensitive depth up to 23 mm. This corresponds to the range of electrons of energy about 10 MeV. Method I is described in detail in ref. <sup>14</sup>), and will not be further discussed here. In Fig 1 a block diagram of Method II is shown, and the Ge(Li)-detector used in Method III is also indicated. The response function and the efficiency of the Si(Li)-system are discussed in Section 2.5. Method III is described in ref. <sup>15</sup>).

### 2.3 Experimental procedures

As no chemical separation was used the mass separated samples contained, in addition to indium, isobaric components consisting of isotopes of cadmium and/or tin. The situation is favourable for the indium isotopes, however, which could in most cases be enhanced by a proper timing of the experiment. For those indium isotopes measured by Method III no problem with contamination arises as the  $\gamma$ -gates are chosen in a well resolved spectrum measured by a Ge(Li)-detector.

Experimentally, it has been found that a counting rate of up to 4000 cps in the main  $\beta$ -detector gives a  $\beta$ -spectrum free from pile-up. This sample strength also gives a suitable counting rate in the  $\gamma$ -detectors. The reactor power was adjusted to give this intensity. Usually,  $(5-10) \times 10^7$   $\beta$ -events were collected in the main detector in order to obtain an accurate Fermi-Kurie (FK) analysis of the coincident  $\beta$ -spectra.

The 0.9 s activity of  $^{129}\text{In}$  will now be discussed as an example of Method II. The daughter  $^{129}\text{Sn}$  has such a long half-life, 134 s, compared to  $^{129}\text{In}$  that no influence is expected with a collection time of 2 s. About 15000 samples were collected and measured during the experiment. The  $\gamma$ -spectrum is shown in Fig 2. A  $\gamma$ -line corresponding to a ground state transition of 2119 keV was chosen as a gate for the  $\beta$ -spectrum (see Fig 4). The accidental

coincidence spectrum obtained by displacing the time window in the coincidence circuit was subtracted, and the true  $\beta$ -pulse spectrum was then transformed to an electron distribution (see Section 2.5).

In Method III the narrow time window makes the accidental coincidence-rate negligible at the counting rates used. In this case also an energy interval close to each  $\beta$ -gate was recorded, the width being chosen to correspond to that of the gate itself. The intensities recorded were subsequently subtracted from the  $\beta$ -spectra coincident with the  $\beta$ -gates to give a background correction.

#### 2.4 Calibration of the $\beta$ -detector

The linearity of the  $\beta$ -detector has been investigated using conversion electrons from  $^{207}\text{Bi}$  and from the daughters of  $^{228}\text{Th}^{14}$ ). These cover the energy interval from 0.5 to 2.6 MeV. Within this interval the main Si(Li)-detector was linear. The electronic system was controlled with a pulse generator and found to be linear at least up to 10 MeV. The maximum deviation from a line defined by the  $^{207}\text{Bi}$  conversion electron peaks was 4 keV in the range 1.68 - 10 MeV.

During the experiments only  $^{207}\text{Bi}$  was used as a calibration source, and a linear fit to the three conversion electron lines was used as a calibration line in the analysis.

The  $Q_{\beta}$ -values  $3.982 \pm 0.009$  of  $^{87}\text{Kr}^{13}$ ) and  $3.54 \pm 0.01$  MeV of  $^{106}\text{Rh}^{18}$ ) were used as check points of the calibration. Our results were for  $^{87}\text{Kr } Q_{\beta} = 3.87 \pm 0.09$  MeV and for  $^{106}\text{Rh } Q_{\beta} = 3.55 \pm 0.07$  MeV<sup>15</sup>), in agreement with the published values.

#### 2.5 Data analysis

The pulse distributions coincident with different  $\gamma$ -gates were analyzed by means of a computer programme in order to determine the end-points of the energy spectra from a Fermi-Kurie plot. In a first step the pulse distribution was transformed to an electronic distribution, and in a second step the FK parameter  $(N/pWF)^{1/2}$  was calculated where  $N$  is the transformed electron intensity,  $p$  and  $W$  are the relativistic electron momentum and energy, respectively, and  $F$  is the Fermi function. A weighted least squares fit to these points gave the  $E_{\beta}^{\text{max}}$  and, by adding the level energy, the total  $\beta$ -decay energy

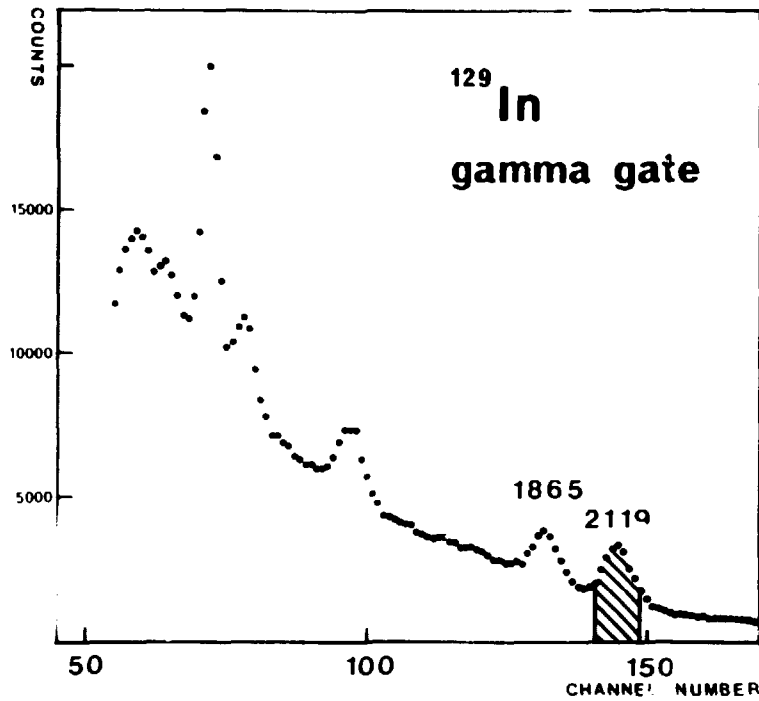


Fig 2. The  $\gamma$ -spectrum of the mass chain 129 recorded with NaI(TL) detectors.

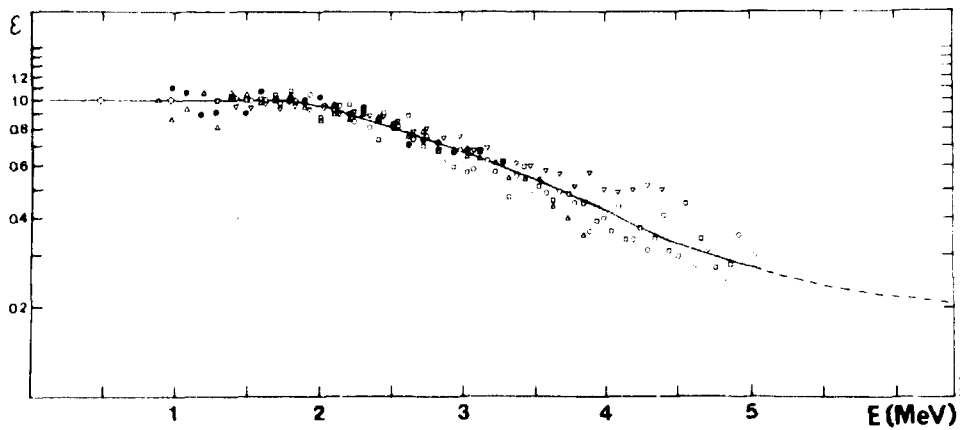


Fig 3. The efficiency function of the Si(Li) system. The experimentally determined points are represented by  $\diamond$  ( $^{207}\text{Bi}$ ),  $\bullet$  ( $^{123}\text{In}$ ),  $\triangle$  ( $^{125}\text{In}$ ),  $\nabla$  ( $^{127}\text{In}$ ),  $\circ$  ( $^{129}\text{In}$ ), and  $\square$  ( $^{125m}\text{In}$ ). The uncertainties of the experimental points around 1.5 MeV, are between 0.05 and 0.07 while an uncertainty between 0.10 and 0.15 is valid for the high energy parts. The solid line represents a fifth degree polynomial fitted to the experimental points.



was deduced.

For the transformation one needs to know the response and the efficiency functions for the  $\beta$ -detector. The response function was determined using the  $^{207}\text{Bi}$  conversion electron spectrum, and a good approximation was found to be a Gaussian full energy peak (FWHM = 12 keV) with a constant tail down to zero energy<sup>15)</sup>. Within the energy range covered, 0.48 - 1.68 MeV, the peak-to-total ratio was found to be 0.30 and independent of electron energy<sup>15)</sup>. Berger et al.<sup>16)</sup> have made an extensive study of the response function for various types of Si(Li)-detectors. They concluded that the peak-to-total ratio was almost constant for energies from 1 to 5 MeV. They also found that the tail down to zero energy was constant even for 5 MeV electrons. In the transformation from pulse distribution to electron distribution a channel width of at least 35-40 keV was chosen. The Gaussian peak then appears in a single channel, which makes the error analysis of the transformation very simple<sup>15)</sup>.

The efficiency function of the  $\beta$ -detector system depends mainly on the anti-coincidence condition but also to a certain extent on the response function used. In the energy range 0.48 to 1.68 MeV the conversion electron spectrum of  $^{207}\text{Bi}$  can be used for an efficiency check. The ratio of the peak intensities for the lines 1681 and 481 keV recorded with our system was  $0.012 \pm 0.001$ , in agreement with 0.012 from ref<sup>17)</sup>. Thus, in this energy range the efficiency was constant.

The odd-mass indium isotopes provide an excellent possibility to determine the efficiency above 1.68 MeV. One can find several coincident  $\beta$ -spectra consisting of only one component. The end-points of these branches are between 3.2 and 5.4 MeV. The experimental  $\beta$ -spectra were transformed with the response function described above and a constant efficiency yielding a first order approximation of  $E_{\beta}^{\text{max}}$ . Using this value a theoretical  $\beta$ -spectrum was calculated, and the ratio between the transformed and the calculated electron distributions gives the efficiency. This procedure was then repeated until no further changes occurred. The resulting efficiency function is shown in Fig 3. For more details see ref.<sup>15)</sup>.

When more than one determination of the  $Q_\beta$ -value of a nuclide were made, the mean value was calculated with its uncertainty given as

$$\sigma = (\bar{\sigma}^2 + \sigma^2(E_{\text{cal}}))^{1/2} \quad (1)$$

where

$$\bar{\sigma} = (\sum_i \sigma_i^{-2})^{-1/2} \quad (2)$$

$\sigma(E_{\text{cal}})$  = the largest calibration uncertainty for the determinations.

The expression (2) was chosen because in all cases it gave values larger than the error deduced from the external consistency of the points. The non-linearity of the system<sup>15)</sup> was found to introduce negligible error (maximum error 4 keV).

### 3. EXPERIMENTAL RESULTS

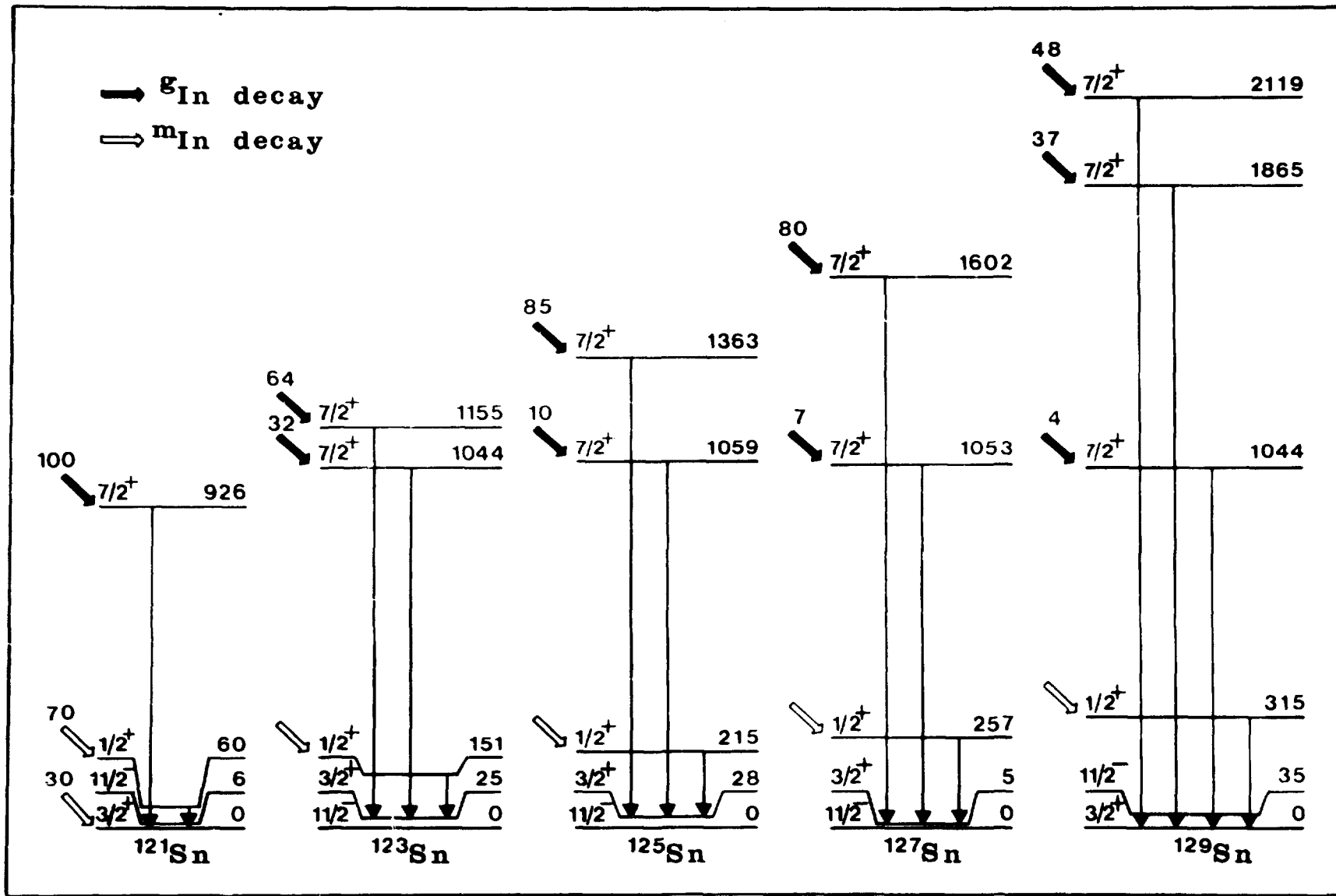
The level structure of tin isotopes has been studied in the mass interval 119 - 132<sup>5-9)</sup>, and the half-lives of the isotopes of indium have been determined by means of  $\beta$ ,  $\gamma$ , and delayed neutron counting<sup>10,11)</sup>.

The present article reports  $Q_\beta$ -values for the complete series from  $^{120}\text{In}$  to  $^{129}\text{In}$ .

#### 3.1 Odd-mass indium isotopes

##### 3.1.1. The nuclides $^{121}\text{In}$ , $^{123}\text{In}$ , and $^{125}\text{In}$

The decay properties of odd-mass indium isotopes in the mass range 119 - 125 have been thoroughly investigated by Fogelberg et al.<sup>5)</sup>. A characteristic feature of these nuclides is the presence of two isomers about 300 keV apart. The spin and parity assignment is  $9/2^+$  for the ground states and  $1/2^-$  for the isomeric states. Partial level schemes of odd-mass tin isotopes from refs.<sup>5,6)</sup> are shown in Fig 4. For determinations of total  $\beta$ -decay energies of the ground states, the  $\gamma$ -transitions 926 keV in  $^{121}\text{Sn}$ , 1020 and 1131 keV in  $^{123}\text{Sn}$ , and 1032 and 1335 keV in  $^{125}\text{Sn}$  were chosen as gates for the  $\beta$ -spectra. These  $\gamma$ -tran-



KAT60906

Fig 4. Partial decay schemes for odd-mass tin isotopes.

sitions depopulate the  $7/2^+$ -states which are strongly favoured (95 - 100 %) in the  $\beta$ -decay. Therefore the coincident  $\beta$ -spectra consist of only one component, which makes a linear fit possible over a wide energy range in the FK analysis.

The isomeric states mainly decay to low-lying states in the daughter nuclei. In  $^{121}\text{Sn}$  the  $1/2^+$  state is situated at 60 keV which is below our limit for  $\gamma$ -gates. The transitions between the  $1/2^+$  and the  $3/2^+$  states in  $^{123}\text{Sn}$  and  $^{125}\text{Sn}$ , of energy 126 and 188 keV, respectively, were chosen as  $\gamma$ -gates for the 1:st forbidden  $\beta$ -spectra from the isomeric states in  $^{123}\text{In}$  and  $^{125}\text{In}$ .

The experimental results are collected in Table 1. The  $Q_{\beta}$ -value is deduced for each  $\beta$ -branch, and for cases where more than one determination is made the average value is calculated.

The main results are the following:

$^{121}\text{g}_{\text{In}}$ :	$Q_{\beta} = 3.41 \pm 0.05 \text{ MeV}$
$^{123}\text{g}_{\text{In}}$ :	$Q_{\beta} = 4.44 \pm 0.06 \text{ MeV}$
$^{123}\text{m}_{\text{In}}$ :	$Q_{\beta} = 4.69 \pm 0.21 \text{ MeV}$
$^{125}\text{g}_{\text{In}}$ :	$Q_{\beta} = 5.48 \pm 0.08 \text{ MeV}$
$^{125}\text{m}_{\text{In}}$ :	$Q_{\beta} = 5.66 \pm 0.12 \text{ MeV}$

The  $Q_{\beta}$ -values for  $^{121}\text{g}_{\text{In}}$  and  $^{123}\text{g}_{\text{In}}$  are in excellent agreement with earlier determinations<sup>18,19</sup>). For  $^{123}\text{In}$  and  $^{125}\text{In}$  the differences between the  $Q_{\beta}$ -values for the isomeric states and the ground states are  $0.25 \pm 0.22 \text{ MeV}$  and  $0.18 \pm 0.14 \text{ MeV}$ , respectively, in agreement with the expected value of about 300 keV.

The FK-plots of  $\beta$ -spectra corresponding to the gates 1335 and 188 keV for the isomers of  $^{125}\text{In}$  are shown in Fig 5.

### 3.1.2 The nuclides $^{127}\text{In}$ and $^{129}\text{In}$

The decay properties of  $^{127}\text{In}$  and  $^{129}\text{In}$ , investigated by de Geer and Holm<sup>6</sup>), are similar to those found for  $^{121,123,125}\text{In}$ . The main  $\beta$ -transition from the ground state of  $^{127}\text{In}$  feeds the level 1602 keV in  $^{127}\text{Sn}$ , while the isomeric state feeds a level at 257 keV. For the  $^{129}\text{In}$  case the analogous levels in  $^{129}\text{Sn}$  are 2119 and 315 keV (see Fig 4).

Table 1

Results of FK analyses for the odd mass indium isotopes  $^{121}\text{In}$ ,  $^{123}\text{In}$ ,  $^{127}\text{In}$ , and  $^{129}\text{In}$ 

Nuclide	Method	Half-life (s)	ref	Gate energy (keV)	Level (keV)	ref	Range of fit (MeV)	$E^{\text{max}}$ (MeV)	$Q_{\beta}$ -value (MeV)	Mean $Q_{\beta}$ -value (MeV)	Other experimental determinations (MeV)
$^{121}\text{gIn}$	I	23.1	a	926	926	b		$2.48 \pm 0.05$	$3.41 \pm 0.05$		$3.38 \pm 0.04^{\text{c}}$
$^{121}\text{mIn}$		233	a						$3.72 \pm 0.05^{\text{d}}$		
$^{123}\text{gIn}$	III	5.98	a	1020	1044	b		$3.36 \pm 0.10$	$4.40 \pm 0.10$	} $4.44 \pm 0.06$	$4.38 \pm 0.05^{\text{e}}$
				1131	1155			$3.30 \pm 0.07$	$4.46 \pm 0.07$		
$^{123}\text{mIn}$	III	47.8	a	126	150	b		$4.54 \pm 0.21$	$4.69 \pm 0.21$		
$^{125}\text{gIn}$	III	2.53	a	1032	1059	b	1.5 - 4.2	$4.34 \pm 0.28$	$5.40 \pm 0.28$	} $5.48 \pm 0.08$	
				1335	1363		1.5 - 4.0	$4.13 \pm 0.08$	$5.49 \pm 0.08$		
$^{125}\text{mIn}$	III	12.2	a	188	215	b	1.2 - 5.2	$5.44 \pm 0.12$	$5.66 \pm 0.12$		
$^{127}\text{gIn}$	II	1.3	a	1597	1602	f		$4.86 \pm 0.08$	$6.46 \pm 0.08$	} $6.49 \pm 0.07$	
				1597	1602			$4.99 \pm 0.16$	$6.59 \pm 0.16$		
$^{127}\text{mIn}$	II	3.7	a	252	257	f		$6.37 \pm 0.28$	$6.63 \pm 0.28$	} $6.65 \pm 0.18$	
				252	257	f		$6.41 \pm 0.24$	$6.67 \pm 0.24$		
$^{129}\text{gIn}$	II	0.9	g	2119	2119	f		$5.48 \pm 0.12$	$7.60 \pm 0.12$		
$^{129}\text{mIn}$	II	1.2	g	315	315	f		$7.5 \pm 0.6$	$7.8 \pm 0.6$		

a) ref 10, b) ref 5, c) ref 18, d) obtained by adding the isomeric transition energy to the  $Q_{\beta}$ -value for  $^{121}\text{gIn}$ .

e) ref 19, f) ref 6, g) ref 6.

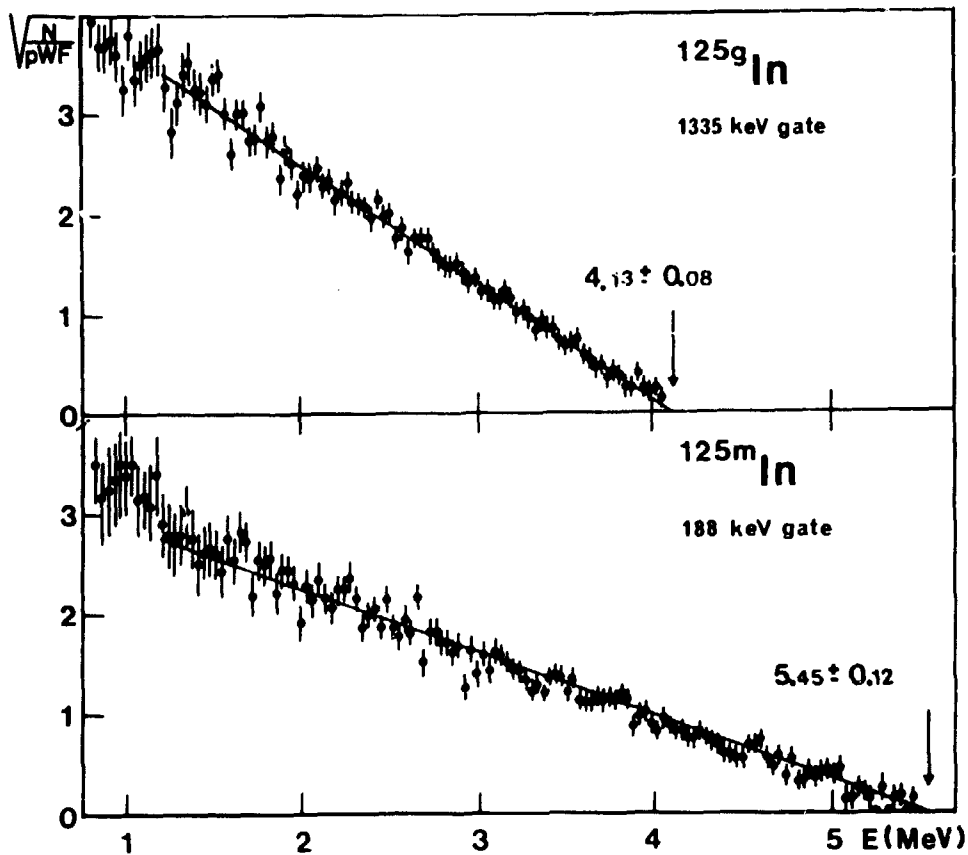


Fig 5. Fermi-Kurie plots of the  $\beta$ -spectra corresponding to the 1335 and 188 keV gates, which depopulate the levels at 1363 and 215 keV in  $^{125}\text{Sn}$ . These levels are fed by  $\beta$ -particles from the ground state and the isomeric state of  $^{125}\text{In}$ , respectively.

The  $\gamma$ -gates and the measured  $\beta$ -end-point energies are given in Table 1. The resulting  $Q_{\beta}$ -values are:

$^{127g}\text{In}$ :	$Q_{\beta} = 6.49 \pm 0.07 \text{ MeV}$
$^{127m}\text{In}$ :	$Q_{\beta} = 6.65 \pm 0.13 \text{ MeV}$
$^{129g}\text{In}$ :	$Q_{\beta} = 7.60 \pm 0.12 \text{ MeV}$
$^{129m}\text{In}$ :	$Q_{\beta} = 7.8 \pm 0.6 \text{ MeV}$

Fermi-Kurie plots of the  $\beta$ -spectra in coincidence with the gates 1597 and 2119 keV in  $^{127}\text{Sn}$  and  $^{129}\text{Sn}$  are shown in Fig 6.

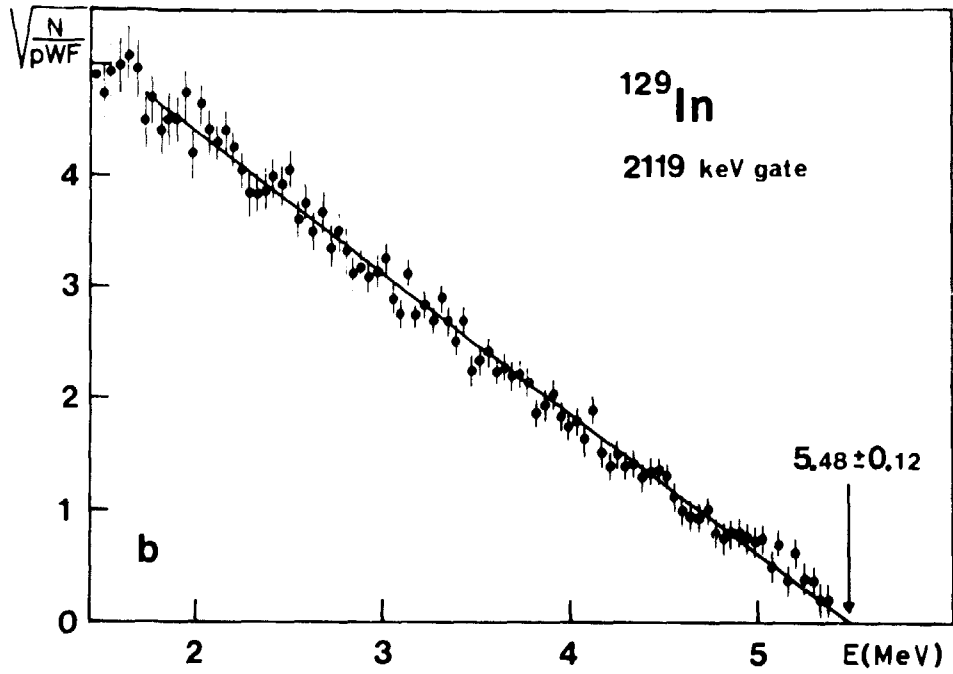
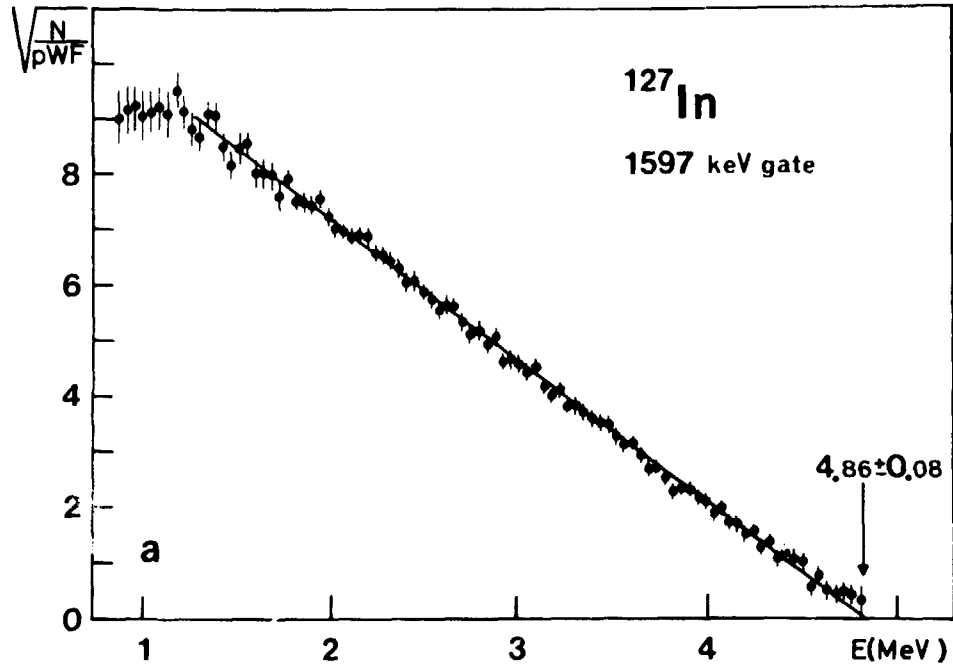


Fig 6. Fermi-Kurie plots of the  $\beta$ -spectra corresponding to the 1597 keV (a) and 2119 keV (b) gates. These  $\beta$ -transitions depopulate the levels at 1602 and 2119 keV in  $^{127}\text{Sn}$  and  $^{129}\text{Sn}$ , respectively.

### 3.2 Even-mass indium isotopes

Investigations of the decay properties of even-mass indium isotopes are in progress<sup>7</sup>). Some pieces of information from these studies and from refs.<sup>20,21</sup>) needed for the discussion below are collected in Fig 7. The situation is similar to that for odd-mass indium isotopes: there are two isomers of indium at all mass numbers from 120 to 128. The  $7^-$ -states in  $^{120-128}\text{Sn}$  are presumably isomeric with a delay of importance for the coincidence experiments<sup>7</sup>).

#### 3.2.1 The nuclide $^{120}\text{In}$

The half-life of the low-spin isomer ( $^{120g}\text{In}$ ) has been determined to be  $3.08\text{ s}$ <sup>23</sup>) and that of the high-spin isomer ( $^{120h}\text{In}$ ) to be  $44\text{ s}$ <sup>20</sup>). The  $3.08\text{ s}$  isomer decays mainly to the ground state of  $^{120}\text{Sn}$  while the feeding of the  $1170\text{ keV}$  level is  $13\%$ <sup>20</sup>). The lowest level fed by  $\beta^-$ -particles from the high-spin isomer is that at  $2195\text{ keV}$ .

Method I was used in the present experiment, and the  $44\text{ s}$  isomer was enhanced by choosing a collection time of  $50\text{ s}$ . Two  $\gamma$ -gates were used:  $1172$  and  $2195\text{ keV}$  (the  $2195\text{ keV}$  gate is a sum peak). Multi-scaling of the decay of the gates shows that only feeding from the long-lived isomer is present in the  $2195\text{ keV}$  gate while also the short-lived component contributes to the  $1172\text{ keV}$  gate.

The  $\beta^-$ -spectrum coincident with the  $1172\text{ keV}$   $\gamma$ -gate is composed by two components with end-points  $4.26 \pm 0.29$  and  $2.48 \pm 0.15\text{ MeV}$ . The range of fit for the high-energy component was  $3.2 - 4.2\text{ MeV}$  which excludes the interference from the long-lived isomer (see level scheme in Fig 7). By adding the gate energy to  $4.26\text{ MeV}$  we obtain the  $Q_{\beta^-}$ -value  $5.43 \pm 0.29\text{ MeV}$  for the low-spin isomer of  $^{120}\text{In}$ .

The  $\beta^-$ -spectrum coincident with the  $2195\text{ keV}$  gate has a single component with an end-point energy of  $3.10 \pm 0.20\text{ MeV}$ . Since this corresponds to the  $\beta^-$ -feeding of the lowest state in the  $44\text{ s}$  decay a  $Q_{\beta^-}$ -value of  $5.30 \pm 0.20\text{ MeV}$  for  $^{120h}\text{In}$  is obtained.

Thus, for the two isomers we get as results

$$^{120g}\text{In}: Q_{\beta^-} = 5.43 \pm 0.29\text{ MeV}$$

$$^{120h}\text{In}: Q_{\beta^-} = 5.30 \pm 0.20\text{ MeV}$$

in agreement with the values  $5.6 \pm 0.6\text{ MeV}$  for the low spin isomer and  $5.3 \pm 0.2\text{ MeV}$  for the high spin isomer obtained by Kantele et al<sup>24</sup>).



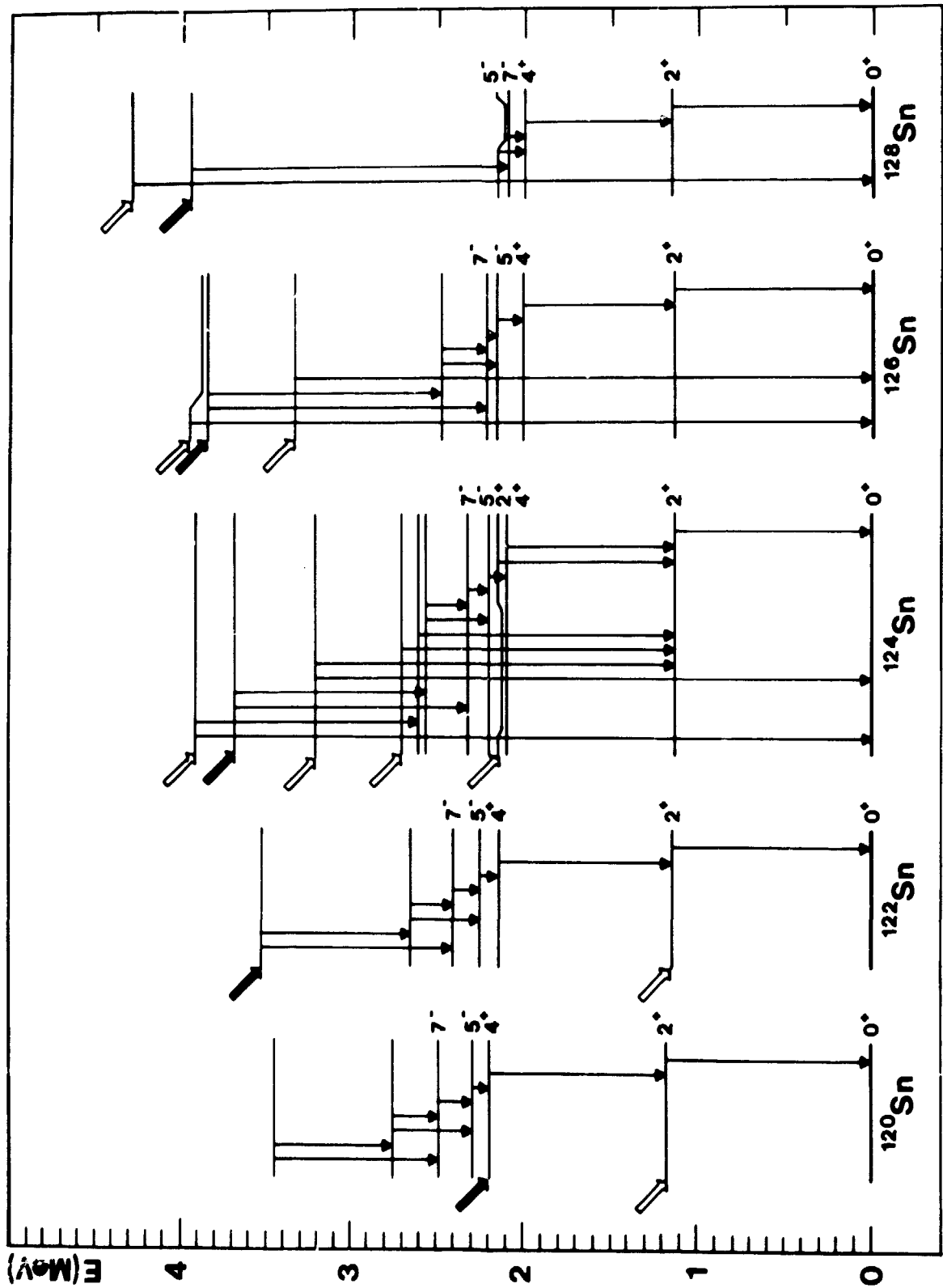


Fig 7. Partial decay schemes for even-mass tin isotopes.

1

Table 2

Results of the FK analyses for even mass indium isotopes  $^{120}\text{In}$ ,  $^{122}\text{In}$ ,  $^{124}\text{In}$ ,  $^{126}\text{In}$ , and  $^{128}\text{In}$ 

Nuclide	Method	Half-life		Gate energy (keV)	Level (keV)		Range of fit (MeV)	$E^{\max}$ (MeV)	$Q_{\beta^-}$ -value (MeV)	Mean $Q_{\beta^-}$ -value (MeV)	Other experimental determinations (MeV)
		(s)	ref			ref					
$^{120}\text{In}$	I	3.08	a	1172	1172	b	3.2 - 4.2	$4.26 \pm 0.29$	$5.43 \pm 0.29$		$5.6 \pm 0.6^c$
$^{120}\text{hIn}$	I	44	a	2195	2195	b		$3.10 \pm 0.20$	$5.30 \pm 0.20$		$5.3 \pm 0.2^c$
$^{122}\text{In}$	III	1.5	d	1141	1141	b	2.9 - 4.5	$5.2 \pm 0.5$	$6.3 \pm 0.5$		$6.5 \pm 0.2^e$
$^{122}\text{hIn}$	III	9.2	d	1122	3531	b	1.2 - 2.5	$2.72 \pm 0.19$	$6.25 \pm 0.19$		$6.6 \pm 0.2^e$
$^{124}\text{In}$	I, III	3.2	f							$7.18 \pm 0.05^g$	
$^{124}\text{hIn}$	III	2.4	f							$7.37 \pm 0.21^g$	
$^{126}\text{In}$	II	2.1	h	3345	3345	h	2.0 - 4.7	$4.84 \pm 0.19$	$8.19 \pm 0.19$	}	$8.17 \pm 0.08$
				3345	3345	h	2.0 - 4.7	$4.88 \pm 0.12$	$8.23 \pm 0.12$		
				3888	3888	h	2.1 - 4.2	$4.23 \pm 0.11$	$8.12 \pm 0.11$		
$^{126}\text{hIn}$	II	1.55	h	1637	3856	h	1.6 - 4.0	$4.20 \pm 0.17$	$8.06 \pm 0.17$		
$^{128}\text{In}$	II	6.5	h	4300	4300	h	1.2 - 4.8	$4.98 \pm 0.18$	$9.28 \pm 0.18$	}	$9.31 \pm 0.16$
				4300	4300	h	2.0 - 4.8	$5.10 \pm 0.34$	$9.40 \pm 0.34$		
$^{128}\text{hIn}$	II	0.95	h	1867	3963	h	1.9 - 5.4	$5.43 \pm 0.22$	$9.39 \pm 0.22$		

a) ref 23   b) ref 20   c) ref 24   d) ref 10   e) ref 21   f) ref 22   g) see table 3   h) ref 7

3.2.2 The nuclide  $^{122}\text{In}$

For  $^{122\text{c}}\text{In}$  (low spin) and  $^{122\text{h}}\text{In}$  (high spin) the half lives have been determined to 1.5 and 9.2 s, respectively<sup>10</sup>).

Using Method III the  $\gamma$ -lines 1122 and 1141 keV, depopulating the levels at 3531 and 1141 keV, were chosen as gates (see Fig 7). The end-points of the  $\beta$ -spectra are given in Table 2. The  $Q_{\beta}$ -values for the two isomers are

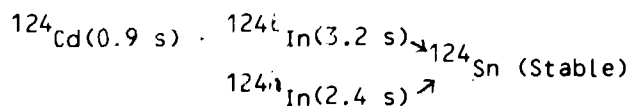
$$^{122\text{c}}\text{In}: Q_{\beta} = 6.3 \pm 0.5 \text{ MeV}$$

$$^{122\text{h}}\text{In}: Q_{\beta} = 6.25 \pm 0.19 \text{ MeV}$$

The values  $6.5 \pm 0.2$  and  $6.6 \pm 0.2$  MeV have been reported for the low and high spin isomers of  $^{122}\text{In}$ <sup>21</sup>).

3.2.3 The nuclide  $^{124}\text{In}$

The nuclide  $^{124}\text{In}$  belongs to the following isobaric chain<sup>7,22</sup>):



The half-lives have been determined by means of  $\gamma$ -counting<sup>22</sup>).

The low-spin isomer is known to decay with feeding to the levels at 2130, 3215, and 3920 keV. The levels at 2571 and 3688 keV are assigned to the decay of  $^{124\text{h}}\text{In}$ .

The  $\gamma$ -transition from the 3215 keV state to the ground state gives rise to a rather strong peak in the  $\gamma$ -spectrum in an energy region where the background is low. It is therefore well suited as a gate using Method I. With the same method a  $\gamma$ -gate was also chosen around 1132 keV, but the situation is here more complicated since double escape peaks from three lines around 2150 keV are also present.

Table 3

Summary of  $Q_{\beta}$ -determination for  $^{124}\text{In}$  ( $T_{1/2}=3.2$  s) and  $^{124}\text{In}$  ( $T_{1/2}=2$  s)

Isomer	Method	Gate energy (keV)	Level (keV)	Range of fit (MeV)	$E_{\beta}^{\text{max}}$ (MeV)	$Q_{\beta}$ -value (MeV)
3.2 s	III	997	2150	2.4 - 5.0	5.10±0.15	7.23±0.1
	III	1315	3920	1.0 - 3.0	3.39±0.26	7.31±0.26
	III	1471	2604	1.4 - 3.1	3.46±0.24	
	III	1572	2705	1.6 - 3.1	3.82±0.66	
	III	2083	3215	0.6 - 3.6	4.01±0.31	7.23±0.31
	III	3215	3215	1.3 - 3.7	3.97±0.16	7.19±0.16
	I	3215	3215	1.6 - 3.6	3.92±0.12	7.14±0.12
	III	2703 <sup>a)</sup>	3215	0.6 - 3.6	3.94±0.25	7.16±0.25
	I	2703 <sup>a)</sup>	3215	2.5 - 3.6	3.94±0.12	7.16±0.12
I	2192 <sup>b)</sup>	3215	2.5 - 3.6	3.92±0.09	7.14±0.09	
Mean value:						7.18±0.05
2 s	III	244	2571	1.0 - 3.1	3.50±0.32	
	III	364	2571	1.5 - 3.2	3.74±0.24	
	III	1118	3688	1.2 - 3.2	3.66±0.32	7.35±0.32
	III	1361	3688	1.6 - 3.3	3.70±0.29	7.39±0.29
Mean value:						7.37±0.21

<sup>a)</sup> Single escape

<sup>b)</sup> Double escape

A second experiment with Method III was performed, and the results of the  $\beta$  end-point energies and the  $\gamma$ -gates are collected in Table 3 together with results obtained with Method I. The  $Q_{\beta}$ -value of the high-spin isomer was obtained by measuring the  $\beta$ -spectrum coincident with  $\gamma$ -transitions from the 3688 keV level. The  $\beta$ -spectra coincident with transitions from the level at 2571 keV had the same  $\beta$  end-point energies as those depopulating the 3688 keV level indicating that the  $\beta$ -particles mainly feed the latter level. The results are collected in Table 3.

The mean values of the  $Q_{\beta}$  determinations are:

$${}^{124}_{\ell}\text{In } Q_{\beta} = 7.18 \pm 0.05 \text{ MeV}$$

$${}^{124}_{h}\text{In } Q_{\beta} = 7.37 \pm 0.21 \text{ MeV}$$

#### 3.2.4 The nuclides ${}^{126}_{\ell}\text{In}$ and ${}^{128}_{\ell}\text{In}$

The half-lives of the different isomers of the nuclides  ${}^{126}_{\ell}\text{In}$  and  ${}^{128}_{\ell}\text{In}$  are given in Table 2. The high-spin isomers were studied by setting  $\gamma$ -gates around the 1637 keV transition depopulating the 3856 keV level in  ${}^{126}_{\ell}\text{In}$  and around the 1867 keV transition depopulating the 3963 keV level in  ${}^{128}_{\ell}\text{In}$ .

In order to increase the coincidence rate for these very short-lived activities the experiments were performed with the Method II. The results from the FK-plots of the various  $\beta$ -spectra are collected in Table 2, and a FK-plot of the  $\beta$ -spectrum corresponding to the gate at 4300 keV in the decay of  ${}^{128}_{\ell}\text{In}$  is shown in Fig 8. The results for the different isomers are:

$${}^{126}_{\ell}\text{In: } Q_{\beta} = 8.17 \pm 0.08 \text{ MeV}$$

$${}^{126}_{h}\text{In: } Q_{\beta} = 8.06 \pm 0.17 \text{ MeV}$$

$${}^{128}_{\ell}\text{In: } Q_{\beta} = 9.31 \pm 0.16 \text{ MeV}$$

$${}^{128}_{h}\text{In: } Q_{\beta} = 9.39 \pm 0.22 \text{ MeV}$$

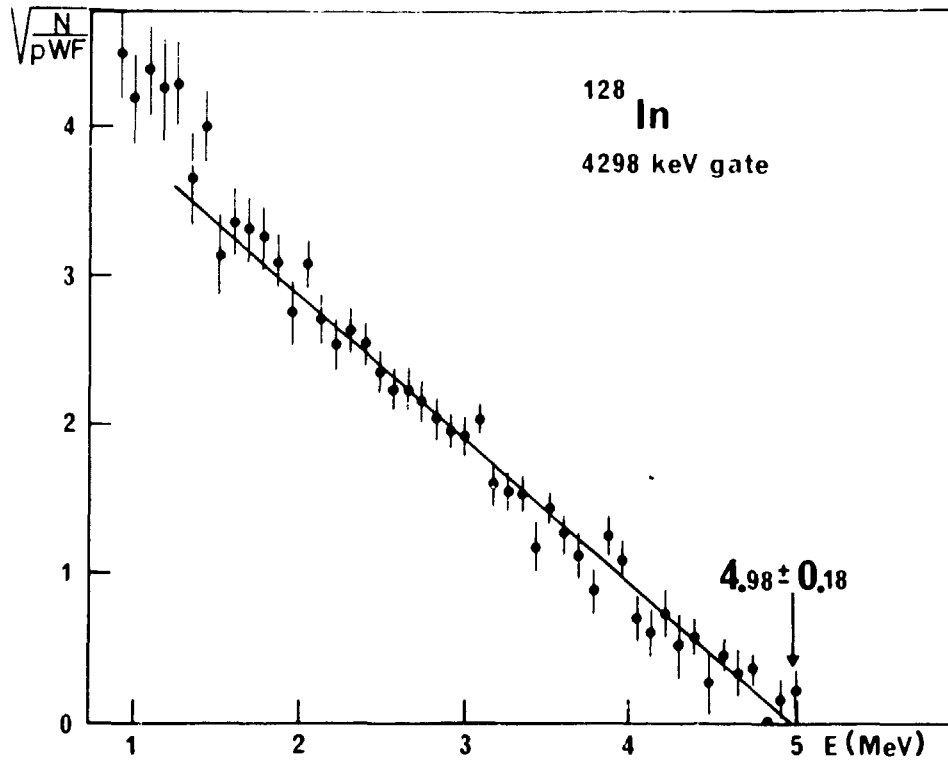


Fig 8. Fermi-Kurie plot of the  $\beta$ -spectrum corresponding to the gate at 4300 keV in the decay of  $^{128}\text{In}$ .

#### 4. DISCUSSION

##### 4.1 $Q_{\beta}$ -values

In the following the  $Q_{\beta}$ -values for the ground states of the odd-mass indium isotopes will be discussed. The results for the even-mass isotopes are not accurate enough to establish the relative position of the isomers. Therefore, the cases where the  $Q_{\beta}$ -figure is lowest have been arbitrarily chosen for the discussion. The low spin isomers of even-mass isotopes are fed in the decay of even-mass cadmium isotopes and, consequently, their mass excesses should be used when determining the mass excesses for those cadmium isotopes by the indirect  $Q_{\beta}$ -method.

In the comparison of the  $Q_{\beta}$ -values with predictions from mass formulae, three different types of formulae are chosen, namely the droplet models of Myers<sup>26a</sup>), Groote et al.<sup>26b</sup>), and Seeger-Howard<sup>26c</sup>), the semi-empirical shell-model of Liran-Zeldes<sup>26d</sup>), and the empirical mass relations of Comay-Kelson<sup>26e</sup>) and Garvey et al.<sup>25</sup>). The experimental values and the corresponding deviation in the predictions are compiled in Table 3. The mean experimental error for the complete series  $^{120-129}\text{In}$  is 0.12 MeV, and the average deviations for the mass formulae used in the comparison vary between 0.17 and 0.67 MeV (see Table 4). The droplet model predictions are less accurate than the others. It should be remembered, however, that fewer coefficients are used than in the other cases.

##### 4.2 Masses

The mass excesses of  $^{120-126}\text{Sn}$  and  $^{127-129}\text{Sn}$  are known from refs.<sup>26f</sup> and <sup>27</sup>), respectively. By adding the  $Q_{\beta}$ -values from Table 4 to these mass excesses, the masses of  $^{120-129}\text{In}$  were deduced (cf. Table 5). The resulting masses are then compared to mass predictions<sup>25,26a-26e</sup>) in Table 6.

The mean experimental error for the indium isotopes studied are 0.12 MeV, and the predictions deviate, on average, by 0.12 to 1.39 MeV. The formulae of Liran-Zeldes, Comay-Kelson, and Garvey et al. give, in general, predictions with acceptable precision. Among the droplet model formulae, the Seeger-Howard one reproduces the experimental masses very well. Before drawing any conclusions about which droplet formula to be used far away from stability we recapitulate the results<sup>27</sup>) from mass determinations of neutron-rich tin, antimony, and tellurium isotopes. For these isotopes Myers gives the best predictions (mean deviation 0.32 MeV) while Seeger-Howard and Groote et al., on the

Table 4

Summary of  $Q_{\beta}$ -values obtained in the present work and comparison with different mass formulae predictions

Nuclide	$Q_{\beta}$ -value (MeV)	$Q_{\beta,exp}$		$Q_{\beta,pred}$		(MeV)	
		a	b	c	d	e	f
$^{120}h_{In}$	$5.30 \pm 0.20$	0.61	0.95	0.47	-0.04	0.06	-0.11
$^{121}g_{In}$	$3.41 \pm 0.05$	0.24	0.36	0.58	-0.21	0.15	-0.13
$^{122}h_{In}$	$6.25 \pm 0.19$	0.58	0.87	0.34	-0.10	0.05	-0.30
$^{123}g_{In}$	$4.44 \pm 0.06$	0.33	0.38	0.41	-0.16	0.20	0.06
$^{124}l_{In}$	$7.18 \pm 0.05$	0.61	0.83	0.29	-0.04	0.12	-0.17
$^{125}g_{In}$	$5.48 \pm 0.08$	0.44	0.43	0.35	-0.01	0.24	0.01
$^{126}h_{In}$	$8.06 \pm 0.17$	0.60	0.75	0.09	0.05	0.10	-0.10
$^{127}g_{In}$	$6.49 \pm 0.07$	0.56	0.48	0.24	0.20	0.27	0.12
$^{128}l_{In}$	$9.31 \pm 0.16$	0.98	1.06	0.44	0.60	0.58	0.39
$^{129}g_{In}$	$7.60 \pm 0.12$	0.80	0.65	0.40	0.62	0.64	0.29
$ Q_{\beta,exp} - Q_{\beta,pred} $		0.57	0.67	0.36	0.20	0.24	0.17

a) ref 26a

d) ref 26d

b) ref 26b

e) ref 26e

c) ref 26c

f) ref 27



Table 5

Compilation of experimental mass excesses for neutron-rich indium isotopes

Nuclide	Mass excess (MeV)	$\beta^-$ -decay	$Q_{\beta^-}$ -value (MeV)	Nuclide	Mass excess (MeV)
$^{120}\text{Sn}$	$-91.100 \pm 0.003^a$	$^{120}\text{In} \rightarrow ^{120}\text{Sn}$	$5.30 \pm 0.20$	$^{120}\text{In}$	$-85.80 \pm 0.20$
$^{121}\text{Sn}$	$-89.201 \pm 0.003^a$	$^{121}\text{In} \rightarrow ^{121}\text{Sn}$	$3.41 \pm 0.05$	$^{121}\text{In}$	$-85.79 \pm 0.05$
$^{122}\text{Sn}$	$-89.944 \pm 0.004^a$	$^{122}\text{In} \rightarrow ^{122}\text{Sn}$	$6.25 \pm 0.19$	$^{122}\text{In}$	$-83.69 \pm 0.19$
$^{123}\text{Sn}$	$-87.819 \pm 0.004^a$	$^{123}\text{In} \rightarrow ^{123}\text{Sn}$	$4.44 \pm 0.06$	$^{123}\text{In}$	$-83.38 \pm 0.06$
$^{124}\text{Sn}$	$-88.239 \pm 0.005^a$	$^{124}\text{In} \rightarrow ^{124}\text{Sn}$	$7.18 \pm 0.05$	$^{124}\text{In}$	$-81.06 \pm 0.05$
$^{125}\text{Sn}$	$-85.899 \pm 0.005^a$	$^{125}\text{In} \rightarrow ^{125}\text{Sn}$	$5.48 \pm 0.08$	$^{125}\text{In}$	$-80.42 \pm 0.08$
$^{126}\text{Sn}$	$-86.022 \pm 0.012^a$	$^{126}\text{In} \rightarrow ^{126}\text{Sn}$	$8.06 \pm 0.17$	$^{126}\text{In}$	$-77.96 \pm 0.17$
$^{127}\text{Sn}$	$-83.509 \pm 0.025^b$	$^{127}\text{In} \rightarrow ^{127}\text{Sn}$	$6.49 \pm 0.07$	$^{127}\text{In}$	$-77.02 \pm 0.07$
$^{128}\text{Sn}$	$-83.31 \pm 0.06^b$	$^{128}\text{In} \rightarrow ^{128}\text{Sn}$	$9.31 \pm 0.16$	$^{128}\text{In}$	$-74.00 \pm 0.17$
$^{129}\text{Sn}$	$-80.63 \pm 0.12^b$	$^{129}\text{In} \rightarrow ^{129}\text{Sn}$	$7.60 \pm 0.12$	$^{129}\text{In}$	$-73.03 \pm 0.17$

a) ref 26f

b) ref 27

average, predict the masses to be 1.0 MeV and 0.87 MeV less bound than found experimentally. Apparently, the estimates using the formula of Groote et al. are less precise both for isotopes with  $Z < 50$  and  $Z \geq 50$ . Myers' predictions are very good for the region  $Z \geq 50$ , but the failure in the predictions for  $^{120-129}\text{In}$  is grave. This leads us to conclude that, as for neutron-rich zinc, gallium, germanium, and arsenic isotopes<sup>28</sup>, the best mass formula for extrapolations far away from stability in the region studied is the one of Seeger and Howard.

Table 6

Summary of experimental mass excesses obtained for  $^{120-129}\text{In}$  and comparisons with different mass formulae predictions

Nuclide	Mass excess (MeV)		$M_{\text{exp}} - M_{\text{pred}}$ (MeV)					
			a	b	c	d	e	f
$^{120}\text{In}$	-85.80	0.20	1.36	1.35	0.50	-0.01	0.18	-0.10
$^{121}\text{In}$	-85.79	0.05	1.36	1.30	0.6	0.04	0.28	-0.17
$^{122}\text{In}$	-83.69	0.19	1.45	1.36	0.21	-0.03	0.22	-0.30
$^{123}\text{In}$	-83.38	0.06	1.44	1.26	0.22	0.04	0.41	-0.02
$^{124}\text{In}$	-81.06	0.05	1.45	1.20	0.04	-0.02	0.25	-0.15
$^{125}\text{In}$	-80.42	0.08	1.46	1.08	0.08	0.12	0.38	0.05
$^{126}\text{In}$	-77.96	0.17	1.33	0.84	-0.46	0.00	0.11	-0.06
$^{127}\text{In}$	-77.02	0.07	1.34	0.69	-0.32	0.19	0.11	0.14
$^{128}\text{In}$	-74.00	0.17	1.49	0.70	-0.30	0.42	0.24	0.33
$^{129}\text{In}$	-73.03	0.17	1.25	0.26	-0.53	0.37	0.05	0.16
$\langle M_{\text{exp}} - M_{\text{pred}} \rangle$			1.39	1.00	0.34	0.12	0.22	0.15

a) ref 26a

b) ref 26b

c) ref 26c

d) ref 26d

e) ref 26e

f) ref 25

Acknowledgements

The authors are grateful to Dr B Fogelberg for submitting to us results prior to publication and for interesting discussions.

This work was supported by the Swedish Council for Atomic Research.

REFERENCES

1. W L Talbert, in Proceedings of the International Conference on the Properties of Nuclei Far from the Region of Beta-Stability, Leysin, 1970, p.109, CERN-70-30 (1970).
2. C Thibault, in Proceedings of the 3rd International Conference on Nuclei far from Stability, Cargèse, 1976, p.93, CERN 76-13 (1976).
3. D N Schram and E B Norman, *ibid.* p. 570.
4. S Borg, I Bergström, G B Holm, B Rydberg, L-E De Geer, G Rudstam, B Grapengiesser, E Lund, and L Westgaard, Nucl. Instr. Methods 91 (1971) 109.
5. B Fogelberg, L-E De Geer, K Fransson, and M af Ugglas, Z. Physik A276 (1976) 381.
6. L-E De Geer and G B Holm, Research Institute for Physics Annual Report (1974) p. 102.
7. B Fogelberg et al., private communication.
8. A Kerek, G B Holm, S Borg, and P Carlé, Nucl. Phys. A209 (1973) 520.
9. A Kerek, G B Holm, L-E De Geer, and S Borg, Phys. Lett. 44B (1973) 252.
10. B Grapengiesser, E Lund, and G Rudstam, J. Inorg. Nucl. Chem. 36 (1974) 2409.
11. E Lund and G Rudstam, Phys. Rev. C13 (1976) 1544.
12. Ch Andersson, B Grapengiesser, and G Rudstam, Proceedings of the 8th International EMIS Conference, Skövde, p. 463 (1973).
13. G Andersson, B Hedin, and G Rudstam, Nucl. Instr. Methods 28 (1964) 245.
14. E Lund and G Rudstam, Nucl. Instr. Methods 133 (1976) 173.
15. K Aleklett, Ph Thesis 1977.
16. M J Berger, S M Seltzer, S E Chappell, J C Humphreys, and J W Motz, Nucl. Instr. Methods 69 (1969) 181.
17. R L Auble, Nuclear Data Sheets 5 (1971) 207.
18. A H Wapstra and N B Gove, Nucl. Data Tables 9 (1971) 267.
19. R L Auble, Nucl. Data Sheets 7 (1972) 363.
20. E Liukkonen and J Hattula, Z. Physik. 241 (1971) 150.
21. K Takahashi, D L Swindle, and P K Kuroda, Phys. Rev. 4 (1971) 517.

22. B Fogelberg, T Nagarajan, and B Grapengiesser, Nucl. Phys. A230 (1974) 214.
23. Ö Scheidemann and E Hagebö, J. Inorg. Nucl. Chemistry 35 (1973) 3055.
24. J Kantele and M Karras, Phys. Rev. 135 (1964) B9.
25. G T Garvey, W J Grace, R L Jaffe, I Talmi, and I Kelson, Revs. Mod. Phys. 41 (1969) S1.
26. Atomic Data and Nuclear Data Tables, Vol. 17, Nr 5-6 (1976)
  - a. W D Myers, p. 411 and LBL-3428 (1974)
  - b. H v Groote, E R Hilf and K Takahashi, p. 418
  - c. P A Seeger and W M Howard, p. 428, and LA-5750 (1974)
  - d. S Liran and N Zeldes, p. 431
  - e. E Comay and I Kelson, p. 463
  - f. A H Wapstra and K Bos, p. 474
27. E Lund, K Aleklett, and G Rudstam, The Swedish Research Councils' Laboratory Report LF-75 (1977).
28. K Aleklett, E Lund, and G Rudstam, The Swedish Research Councils' Laboratory Report LF-74 (1977).

